Polymer 51 (2010) 3039–3046

Contents lists available at ScienceDirect

Polymer

journal homepage: www.elsevier.com/locate/polymer

Preparation of block-brush PEG-*b*-P(NIPAM-*g*-DMAEMA) and its dual stimulus-response

Bo-Yu Zhang, Wei-Dong He*, Wen-Tao Li, Li-Ying Li, Ke-Ren Zhang, Hao Zhang

Department of Polymer Science and Engineering, CAS Key Laboratory of Soft Matter Chemistry, University of Science and Technology of China, Hefei, Anhui 230026, China

ARTICLE INFO

Article history:
Received 11 March 2010
Received in revised form
4 May 2010
Accepted 7 May 2010
Available online 15 May 2010

Keywords:
Stimulus response
Block -brush copolymers
ATRP

ABSTRACT

Well-defined dually responsive block-brush copolymer of poly(ethylene glycol)-*b*-[poly(*N*-isopropylacrylamide)-*g*-poly(*N*,*N*-dimethylamino-ethylmethacrylate)], [PEG-*b*-P(NIPAM-*g*-PDMAEMA)] was successfully prepared by the combination of atom transfer radical polymerization (ATRP) and click chemistry based on azide-capped PDMAEMA and alkyne-pending PEG-*b*-PNIPAM copolymer. Azide-capped PDMAEMA was synthesized through ATRP of DMAEMA monomer using an azide-functionalized initiator of β-azidoethyl-2-bromoisobutyrate. Alkyne-pending PEG-*b*-PNIPAM copolymer was obtained through ATRP copolymerization of NIPAM with propargyl acrylate. The final block-brush copolymer was synthesized by the click reaction between these two polymer precursors. Because of characteristics of three different blocks, the copolymer exhibited dually thermo- and pH-responsive behavior. The responsive behaviors of block-brush copolymer were studied by laser light scattering, temperature-dependent turbidity measurement and micro differential scanning calorimetry. The phase transition temperature of block-brush copolymer increased with the decrease of pH value. At pH = 5.0, the copolymer displayed weak thermo-responsive behavior and might form uni-molecular micelles upon heating. At higher pH values, the block-brush copolymer aggregated intermolecularly into the micelles during the phase transition.

1. Introduction

The macromolecular architecture of copolymers determines the macroscopic properties of polymeric materials. Well-defined segmented copolymers such as block and graft polymers which have different functionalized chains, could self-assemble into various micellar structure in segment-selective solvents and have attracted great interests in physical chemistry and polymer science [1–6]. Some amphiphilic block copolymers such as polystyrene-*b*-poly(ethylene oxide) [7] and poly(2-vinylpyridine)-*b*-poly(ethylene oxide) [8] could form various morphologic core-shell micelles. Copolymers consisting of two or more different polymeric blocks, such as poly(*N*-isopropylacrylamide) (PNIPAM) and poly(acrylic acid), exhibit stimulus-response behavior at different temperatures and pHs, which have potential to be used as the carriers for gene and drug delivery [9]. Besides block copolymers, graft or brush copolymers exhibit the similar behavior, with the additional facts that the branched structure makes the micellization more complicated than block copolymers and provides the micelles with more extra properties and applications [10]. Thus, well-defined block-brush copolymer would combine the advantages of both block and graft polymer, such as distinct physicochemical attributions and lower melting viscosity for a given molecular weight [11]. Secondly, the linear triblock copolymer usually has low steric hindrance and electric repulsion; each block could exhibit the individual nature of polymer chain. On the contrary, block-brush copolymers could have different solution properties and assembly behavior from linear block copolymer due to the stronger interaction among the blocks.

Using living/controlled radical polymerizations, such as atom transfer radical polymerization (ATRP) [12] and reversible addition-fragmentation chain transfer polymerization [13], well-defined polymers could be easily synthesized. One of conventional ideas for the preparation of regular branched copolymer is the usage of macromonomers [14,15]. Although ATRP method could be employed for some macromonomers, it inherently possesses a lower reactivity because of steric hindrance and needs to adopt small molecular ATRP initiator [16]. It seems hard to prepare block-brush copolymer from the living/controlled polymerizations of macromonomer with macroinitiator. Combined with other chemical reactions having high efficiency and quantitative yield, such as click chemistry (i.e. 1,3-dpolar cycloaddition of [3 + 2] system)

* Corresponding author. Tel.: +86 551 3601699; fax: +86 551 3606743.
E-mail address: wdhe@ustc.edu.cn (W.-D. He).

0032-3861/$ – see front matter © 2010 Elsevier Ltd. All rights reserved.
doi:10.1016/j.polymer.2010.05.012

[17,18], not only the controlled molecular weight and high monodispersity have been achieved [19], but also polymers with more complex architectures have been obtained. The macromolecules with various architectures such as star block copolymers [20,21], comb-like copolymers [22], H-shape copolymers [23] and theta-shape copolymers [24] have been synthesized. So this methodology could also be extended to the preparation of well-defined block-brush copolymer.

Poly(ethylene glycol) (PEG) has been popularly used as the water-soluble block in constructing the copolymers because of its biocompatibility and physicochemical properties [25]. Poly(*N*-isopropylacrylamide) (PNIPAM) is a wildly-used thermal responsive polymer [26]. There are a lot of research reports on the thermo-dependent micellization of PEG/PNIPAM copolymers [27–29]. Poly(*N*,*N*-dimethylaminoethyl methacrylate) (PDMAEMA) is a weak base with p*K*a about 7.0 and is water-soluble within wide pH range. It shows pH-responsive behavior due to the protonation of the tertiary amine group [30]. The diblock copolymer of PEG-*b*-PDMAEMA shows a potential for application in gene delivery system [31] and encapsulation of antiparasitic compounds for the treatment of leishmaniasis [32]. Recent research reports show that the combination of different functions within a single polymer can contribute to an overall improvement of carrier efficiency [33]. Combination of PEG, PNIPAM and PDMAEMA would offer thermal and pH dual response, and good efficiency in the controlled drug delivery system.

This study aims to the synthesis of well-defined block-brush copolymer, poly(ethylene glycol)-*b*-poly[*N*-isopropylacrylamide-*g*-*N*, *N*-dimethylaminoethyl methacrylate] [PEG-*b*-P(NIPAM-*g*-DMAEMA)] and the fundamental investigation of its dual response.

2. Experimental

2.1. Materials

Methoxy poly(ethylene glycol) (PEG) ($M_n = 5000$, BASF) was dried over anhydrous toluene by azeotropic distillation. Acryloyl chloride was purified by vacuum distillation. *N*-isopropylacrylamide (NIPAM, Kohjin Co., Japan) was purified by recrystallization from a benzene/*n*-hexane mixture (65/35 v/v). 2-Dimethylaminoethyl methacrylate (DMAEMA, Aldrich) was passed through basic alumina column, then vacuum-distilled over CaH_2 prior to use. *N*, *N*, *N*′, *N*″, *N*‴, *N*‴-Hexamethyltriethylenetetramine (Me6TREN) was synthesized according to the method previously described [34]. 2-Chloropropionyl chloride (CPC) and *N*, *N*, *N*′, *N*′, *N*″-pentamethyldiethylenetriamine (PMDETA) were purchased form Alfa Aesar and used without further purification. Triethylamine was stirred with KOH for 12 h at room temperature, refluxed with toluene-4-sulfonyl-chloride and distilled before use. Copper (I) chloride and copper (I) bromide were washed with glacial acetic acid, followed by washing with methanol and ethyl ether to remove impurities, and then dried under vacuum and kept under N_2 atmosphere. THF was dried over sodium/benzophenone and distilled just before use. All other reagents were of analytical grade and used as received. The azide-functionalized ATRP initiator of β-azidoethyl 2-bromoisobutyrate (AEBIB) was synthesized according to our previous report [35].

2.2. Synthesis of 2-chloropropionylated PEG (PEG-Cl)

A solution of PEG (10.00 g, 2 mmol), triethylamine (2.02 g, 20 mmol) and toluene (100 mL) were cooled in an ice-water bath. After 2-chloropropionyl chloride (2.52 g, 20 mmol) was added dropwise in 20 min, the mixture was stirred at room temperature for 12 h. The produced solid was removed by vacuum filtration. After the removal of most solvent by rotary evaporation, the filtrate was precipitated in cold diethyl ether. PEG-Cl was collected by filtration and dried at room temperature under vacuum for 24 h (7.9 g, yield: 79%). The end-group functionality was determined by proton nuclear magnetic resonance (^{1}H NMR) spectroscopy and reached the unity.

2.3. Preparation of PEG-b-P(NIPAM-co-ProA) copolymer by ATRP method

A solution of propargyl alcohol (2.00 g, 0.49 mol), triethylamine (5.50 g, 0.05 mol), hydroquinone (0.050 g) and THF (100 mL) was cooled in ice-water bath. Acryloyl chloride (4.80 g, 0.05 mol) was added dropwise in 20 min. The mixture was stirred in ice-water bath for 1 h and at room temperature for 15 h. After the salt of triethylammonium chloride was filtered off, the solvent was removed by rotary evaporation. Then, propargyl acrylate (ProA) was obtained by further vacuum distillation (4.30 g, yield: 82%).

^{1}H NMR spectroscopy ($CDCl_3$, δ, ppm): 2.45 (*s*, 1H, −C≡C***H***), 4.63 (*s*, 2H, −OC***H***$_2$−C≡CH), 5.85 (*d*, 1H, C***H***$_2$=CH−), 6.10 (*q*, 1H, C***H***$_2$=CH−), 6.34 (*d*, 1H, CH_2 = C***H***−).

Copolymer of PEG-*b*-P(NIPAM-*co*-ProA) with low ProA content was synthesized via ATRP copolymerization of NIPAM and ProA using PEG-Cl as ATRP macro-initiator. NIPAM (1.13 g, 10.0 mmol), PEG-Cl (0.25 g, 0.05 mmol), ProA (27 mg, 0.25 mmol) and DMF (4.0 mL) were added into a polymerization vial equipped with a magnetic stirring bar. After NIPAM and PEG-Cl were completely dissolved, the mixture was frozen. Then, Me6TREN (0.028 g, 0.1 mmol) and CuCl (10 mg, 0.1 mmol) in water (2.0 mL) were added. The mixture was degassed by three freeze–pump–thaw cycles. After the vial was sealed under vacuum, the polymerization reaction was allowed to proceed under stirring at 25 °C. After 10 h, the vial was opened and the reaction mixture was diluted with THF. The thinned mixture was passed through an activated basic Al_2O_3 column to remove copper complex. After removing most THF by rotary evaporation and precipitating the solution in diethyl ether, the product of PEG-*b*-P(NIPAM-*co*-ProA) was collected by filtration and dried under vacuum at room temperature for 24 h (1.10 g, yield 81%). The chemical composition was determined by ^{1}H NMR spectroscopy and relative molecular weight was characterized by gel permeation chromatograph (GPC).

2.4. Synthesis of azide end-functionalized PDMAEMA (PDMAEMA-N_3)

The azide end-functionalized PDMAEMA was synthesized by using AEBIB as ATRP initiator. DMAEMA (3.00 g, 19 mmol), AEBIB (55.6 mg, 0.24 mmol), PMDETA (36.7 mg, 0.24 mmol), CuBr (30.6 mg, 024 mmol) and isopropanol (4.0 mL) were added into a 10-mL polymerization vial. After three freeze–vacuum–thaw cycles, the vial was sealed under vacuum and immersed in a water bath thermostat at 50 °C. After 8 h, the vial was opened. The reaction mixture was diluted with THF and passed through an Al_2O_3 column to remove Cu complex. After most THF was removed by rotary evaporation, the polymer of PDMAEMA-N_3 was obtained by precipitation into hexane and dried in a vacuum oven at 25 °C for 24 h (2.1 g, yield: 70%). The chemical structure was determined by ^{1}H NMR spectroscopy and relative molecular weight was characterized by GPC.

2.5. Synthesis of PEG-b-P(NIPAM-g-DMAEMA) block-brush copolymer

Block-brush copolymer of PEG-*b*-P(NIPAM-*g*-DMAEMA) was synthesized through the cycloaddition reaction between the alkyne

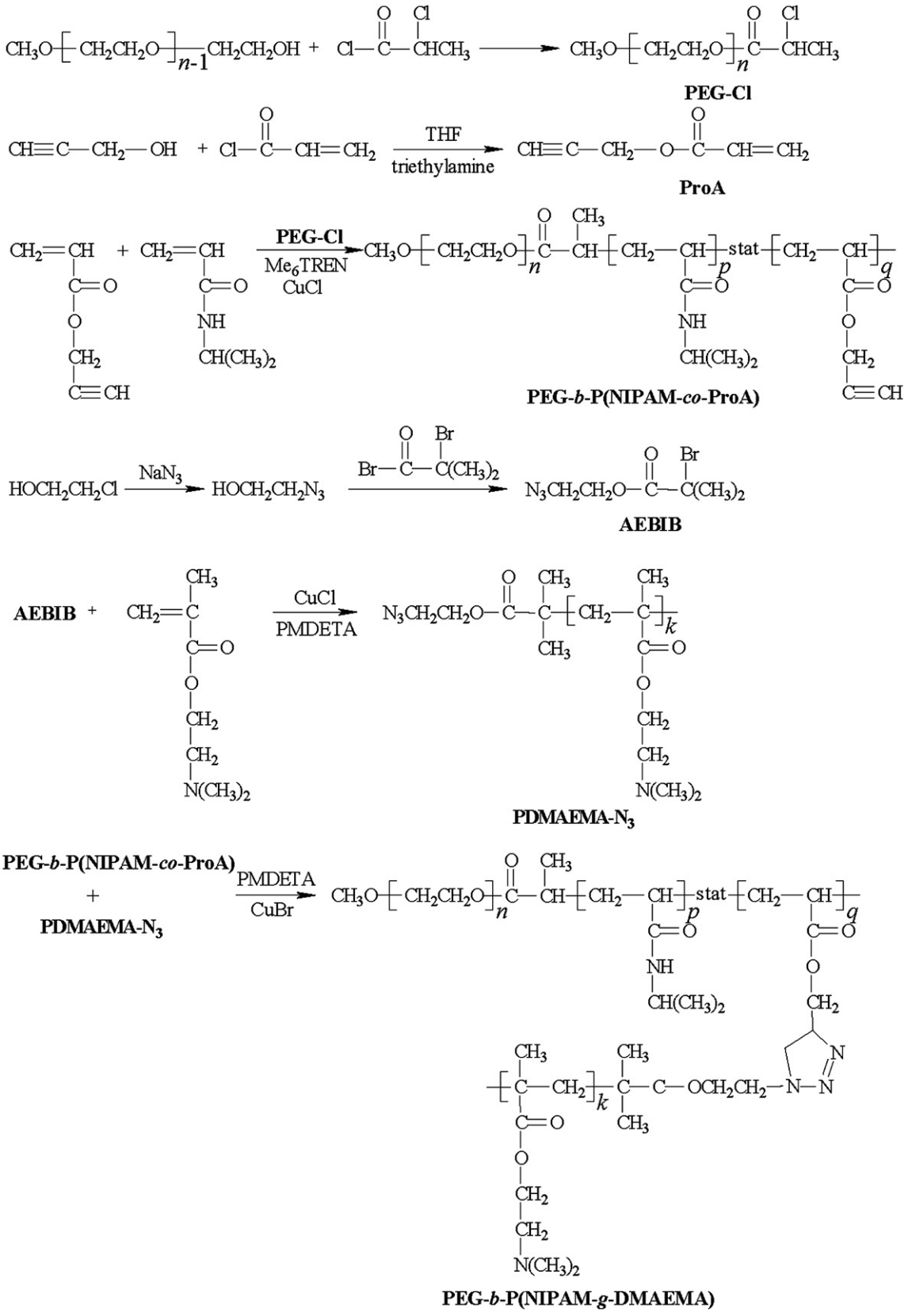

Scheme 1. Schematic illustration of the synthesis of block-brush copolymer of PEG-*b*-P(NIPAM-*g*-DMAMEA).

side-groups of PEG-*b*-P(NIPAM-*co*-ProA) and the azide end-group of PDMAEMA-N_3. Thus, PEG-*b*-P(NIPAM-*g*-DMAEMA) (0.50 g), PDMAEMA (1.13 g), CuBr (13 mg), PMDETA (16 mg) and DMF (6.0 mL) were added into a 10-mL vial. Then the reaction mixture was degassed by three freeze–pump–thaw cycles. The tube was sealed under vacuum and the click reaction was allowed to proceed under vigorous stirring at 30 °C. After 48 h, the reaction was stopped and the mixture was dialyzed against deionized water using a dialysis membrane (cutoff molecular weight: 14,000) for 48 h, and subsequent lyophilized in a freeze drier (SIMENS FD5-3, Germany) for 48 h. Thus, PEG-*b*-P(NIPAM-*g*-DMAEMA) was obtained, and its chemical composition and relative molecular weigh was determined by ^{1}H NMR spectroscopy and GPC, respectively.

2.6. Characterizations

The relative molecular weight and its distribution were determined on a Waters 150C Gel Permeation Chromatography (GPC) equipped with Waters 1515 HPLC pump, Waters 2414 differentia refractive index detector and three Ultrastyragel columns (500, 10^3 and 10^4 A° in series) at 30 °C, using monodispersed polystyrene as calibration standard. DMF was used as eluent at a flow rate of 1.0 mL/min.

^{1}H NMR spectroscopy (300 MHz) measurement for chemical structure and M_{nNMR} was performed on Bruker DMX300 spectrometer in $CDCl_3$. For the investigation of thermal response by NMR, neutral D_2O was used as the solvent. Fourier transform infrared (FTIR) spectra were recorded on a Bruker VECTOR-22 IR spectrometer in KBr pellets.

The optical transmittance of PEG-*b*-P(NIPAM-*g*-DMAEMA) aqueous solution at a wavelength of 500 nm was acquired on a Unico UV/vis 2802PCS spectrophotometer. A thermostatically controlled cuvette was employed. The lower critical solution temperature (LCST) was defined as the temperature corresponding to the initial abrupt decrease in transmittance. The polymer concentration was 2.0 mg/mL.

Micro-DSC measurements were carried out on a VP DSC from MicroCal. The volume of the sample cell is 0.509 mL. The reference cell was filled with deionized water. The sample solution at 2.0 mg/mL was degassed at 25 °C for 0.5 h and equilibrated at 10 °C for 2 h before the heating process at the heating rate of 1.0 °C/min.

Dynamic laser light scattering (DLS) study was performed on a modified commercial laser light scattering spectrometer (ALV/SP-125) equipped with an ALV-5000 multi-τ digital time correlator and a He–Ne laser (output power = 10 mW, λ = 632 nm). Before DLS measurement, the solutions were dust-freed with a Millipore filter (0.45 μm). Scattered light was collected at a fixed angle of 30° for duration of 10 min. All data were averaged over three measurements.

3. Results and discussion

The block-brush copolymer of PEG-*b*-P(NIPAM-*g*-DMAEMA) was synthesized as shown in Scheme 1. Herein, we synthesized PEG-*b*-P(NIPAM-*co*-ProA) having alkyne side-groups and PDMAEMA-N_3 having azide end-group separately by ATRP polymerization, and then obtained PEG-*b*-P(NIPAM-*g*-DMAEMA) through click chemistry.

3.1. Synthesis of PEG-b-P(NIPAM-co-ProA)

Firstly, 2-chloropropionylated PEG as ATRP macro-initiator was synthesized according to the literature [36] and its NMR spectrum is shown in Fig. 1a. The signal of *e* at 1.7 ppm is described to the methyl group originated from the 2-chloropropionyl group, and that of *d* at 3.4 ppm to the methyl group from methoxy PEG. The esterification conversion could be estimated from the relative integral values of the signals of *e* and *d*. The ratio of *e*:*d* is close to 1, indicating the complete conversion of the hydroxyl group of PEG.

In the second step, PEG-*b*-P(NIPAM-*co*-ProA) with low alkyne content was synthesized through ATRP copolymerization of NIPAM and propargyl acrylate with using 2-chloropropionylated PEG as macro-initiator. The polymerization of NIPAM, using PEG-Cl/CuBr/$CuBr_2$/ME_6TREN as the initiator/catalyst system in DMF/H_2O (2/1, V/V) at 25 °C, is well controlled [37]. ^{1}H NMR spectrum of PEG-*b*-P(NIPAM-*co*-ProA) is shown as Fig. 1b. The copolymer composition is determined by comparing the integration of PEG peak (*a*) at 3.7 ppm, NIPAM peak (*b*) at 4.0 ppm and ProA peak (*c*) at 4.7 ppm. The unit ratio of EG:NIPAM:ProA and number-averaged molecular weight by NMR (M_{nNMR}) are listed in Table 1. GPC trace of PEG-*b*-P(NIPAM-*co*-ProA) is shown in Fig. 2, indicating a monomodal and symmetrical elution peak with M_{nGPC} of 29,700 and M_w/M_n of 1.09.

3.2. Preparation of PDMAEMA-N_3

^{1}H NMR spectrum of PDMAEMA-N_3 is shown in Fig. 1c. The peaks at 4.03 (*b*), 2.59 (*c*), 2.27 (*d*), 1.67–2.12 (*e*) and 0.71–1.26 (*f*) ppm are the characteristic signals of PDMAEMA. The peak (*a*) at 3.46 ppm corresponds to the signal of the methylene protons originating from the used initiator. By comparing the integration of the peaks at 3.46 and 4.03 ppm, the polymerization degree of PDMAEMA-N_3 is 80.

IR analysis of PDMAEMA-N_3 shows an absorption peak at 2100 cm^{-1}, which corresponds to the asymmetric stretching vibration of the azide group (Fig. 3). This confirms the successful synthesis of the azide end-functionalized PDMAEMA. The GPC trace of PDMAEMA-N_3 (Fig. 2) also shows narrow and symmetrical molecular distribution (M_w/M_n = 1.15).

3.3. Click reaction between PEG-b-P(NIPAM-co-ProA) and PDMAEMA-N_3

Block-brush copolymer of PEG-*b*-P(NIPAM-*g*-DMAEMA) was obtained through the click reaction between the alkyne side-groups of PEG-*b*-P(NIPAM-*co*-ProA) and the azide end-group of PDMAEMA-N_3. Usually, we used alkyne-functionalized solid support to remove the remaining azide-functionalized polymer as our previous report [35]. However, because the molar ratio of azide group to alkyne group was unity at the present work, we acquired pure PEG-*b*-P(NIPAM-*g*-DMAEMA) without any precursor PDMAEMA-N_3 after the dialysis.

Fig. 3 shows FTIR spectrum of the block-brush PEG-*b*-P(NIPAM-*g*-DMAEMA) after click reaction. The characteristic absorbance of azide group (2106 cm^{-1}) absolutely disappears, indicating the full conversion of PDMAEMA-N_3. GPC trace of PEG-*b*-P(NIPAM-*g*-DMAEMA) is shown in Fig. 2 and shifts to higher molecular weight compared with those of PEG-*b*-P(NIPAM-*co*-ProA) and PDMAEMA-N_3, and its polydispersity becomes a little broader. However, it still keeps unimodal and is free from the tailing in both lower and higher molecular weight region. The result reveals that no residue of PEG-*b*-P(NIPAM-*co*-ProA) or PDMAEMA-N_3 remains after the click reaction and dialysis. The number-averaged molecular weight measured by GPC (M_{nGPC}, 65,400) using polystyrene standards is lower than that by ^{1}H NMR (M_{nNMR}, 91,400), reflecting that the block-brush copolymers possess smaller hydrodynamic volume than the linear analogue [38,39].

^{1}H NMR spectrum of PEG-*b*-P(NIPAM-*g*-DMAEMA) displays the characteristic signals of PEG, PNIPAM and PDMAMEA, as shown in Fig. 1d. Furthermore, the integration ratio of PDMAEMA signal (*d*) at

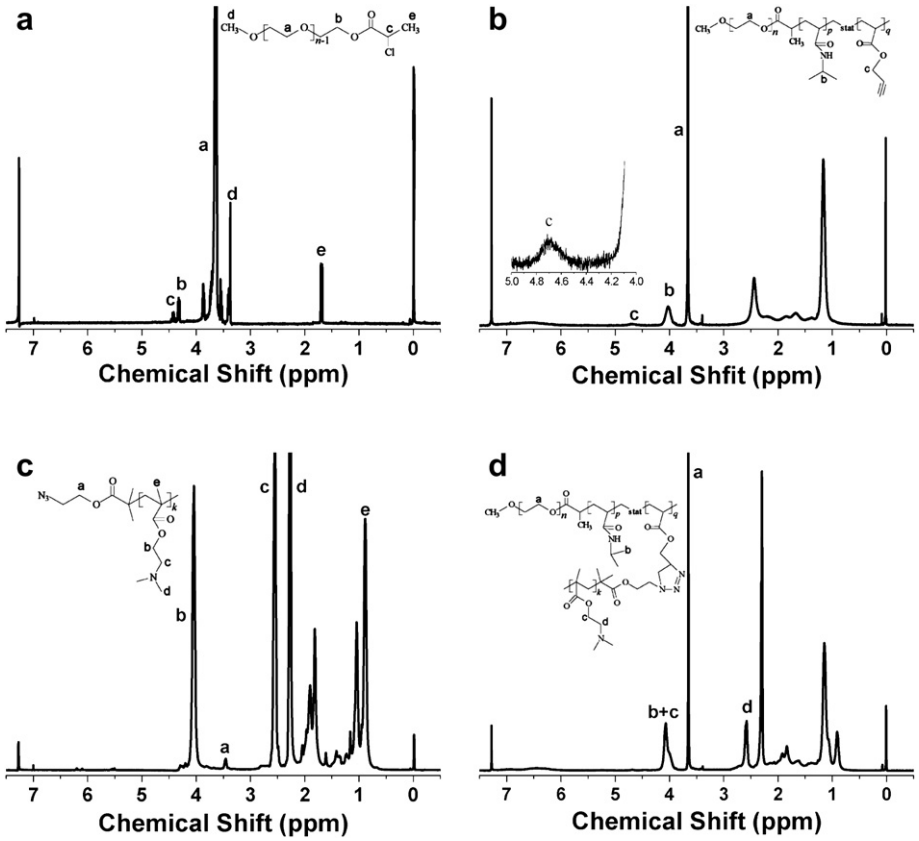

Fig. 1. ^{1}H NMR spectra of PEG-Cl (a), PEG-*b*-P(NIPAM-*co*-ProA) (b), PDMAEMA-N_3 (c) and PEG-*b*-P(NIPAM-*g*-PDMAEMA) (d) in $CDCl_3$.

2.59 ppm to that of the signal (*b* and *c*) of PNIPAM and PDMAEMA at 4.06 ppm is determined to be 0.8, which is the same as the expected value based on the charged amount. By the combination of GPC result, we could conclude that each PDMAEMA-N_3 chain has been successfully stuck to the backbone. M_{nNMR} of PEG-*b*-P(NIPAM-*g*-DMAEMA) was calculated according to the integration values of PEG signal (*a*), PNIPAM signal (*d*) and PDMAEMA signal ($b + c$) and the result is listed in Table 1.

3.4. Stimulus-response behavior of PEG-b-P(NIPAM-g-DMAEMA)

It is well known that PNIPAM homopolymer is temperature-responsive and its LCST in aqueous solution is 32 °C [40]. PDMAEMA homopolymer has LCST varied from 40 to 50 °C with decreasing molecular weight and its LCST value strongly depends on the ionization of the dimethylamino group [41]. However, for the block copolymers composed of PNIPAM and PDMAEMA, the thermal responsive behavior concerning with PDMAEMA block was not observed [42–44]. In our current study, the thermal-sensitive behavior to PNIPAM block and the influence of cationic PDMAEMA block at different pHs are focused. Thermal and pH dual responsive behavior of PEG-*b*-P(NIPAM-*g*-DMAEMA) is investigated by the combination of ^{1}H NMR analysis at different temperatures, dynamic light scattering, temperature-dependent turbidimetry study and micro-DSC.

^{1}H NMR spectra of block-brush PEG-*b*-P(NIPAM-*g*-DMAEMA) with D_2O as the solvent at two temperatures are shown in Fig. 4. PEG-*b*-P(NIPAM-*g*-DMAEMA) is well dissolved at 25 °C and all proton signals are normally observed. Compared with ^{1}H NMR

Table 1
Molecular characterizations of different polymers in this study.

Polymer	NMR result		GPC result	
	Molar ratio of units	M_{nNMR}	M_{nGPC}	M_w/M_n
PEG-Cl	EG:2-CPC = 113:1	5100	5100	1.02
PEG-b-P(NIPAM-*co*-ProA)	EG:NIPAM:ProA = 113:200:5	28,200	29,700	1.09
PDMAEMA-N_3	DMAEMA:AEBIB = 80:1	12,500	12,900	1.15
PEG-*b*-(PNIPAM-*g*-PDMAEMA)	EG:NIPAM:DMAEMA = 113:199:393	91,400	65,400	1.37

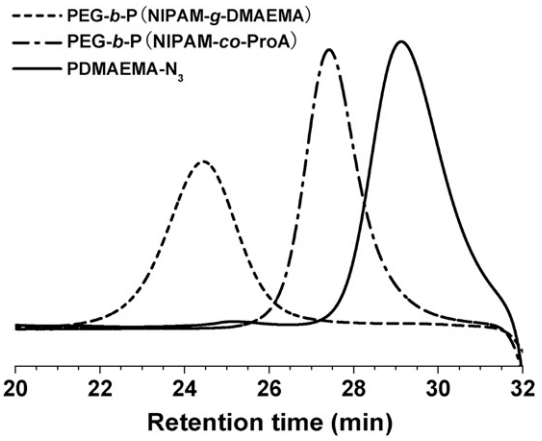

Fig. 2. GPC traces of PDMAEMA-N_3, PEG-*b*-P(NIPAM-*co*-ProA) and PEG-*b*-P(NIPAM-*g*-DMAEMA).

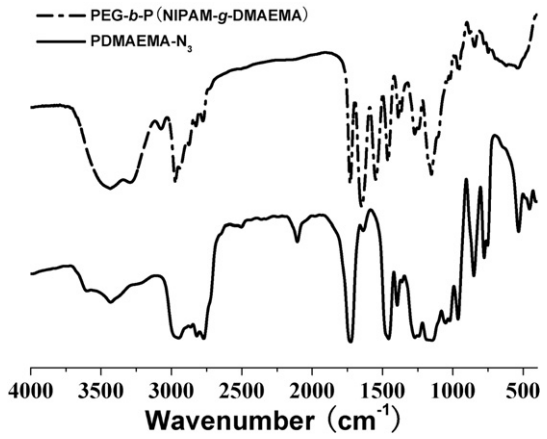

Fig. 3. FTIR spectra of the PDMEAME-N_3 and PEG-*b*-P(NIPAM-*g*-DMAEMA).

spectra with $CDCl_3$ as the solvent, the main change is the separation of the signals of $C\underline{H}(CH_3)_2$ in NIPAM (*b*, 3.97 ppm) and $OC\underline{H}_2$ in DMAEMA (*c*, 4.25 ppm). Other assignments of the concerning protons and the relative integration of the proton signals based on methylene protons of EG unit are summarized in Table 2.

When the solution is heated to 40 °C, PNIPAM chain is dehydrated and collapsed, leading to the variation in ^{1}H NMR spectrum of PEG-*b*-P(NIPAM-*g*-DMAEMA) as shown in Fig. 4 and Table 2. The chemical shift of $C\underline{H}(CH_3)_2$ in NIPAM (*b*) decreases obviously while others in NIPAM hardly change when the temperature rises to 40 °C, resulting from the rupture of hydrogen-bonding of NIPAM amide groups with water, which decreases the hydrophilicity of PNIPAM chains. Furthermore, the integration ratio of $C\underline{H}(CH_3)_2$ in NIPAM (*b*) to PEG signal (*a*) at 3.75 ppm reduces about 46% while the integration ratio of $OC\underline{H}_2$ in DMAEMA (*c*) is almost unchanged. This evidence means that PEG-*b*-P(NIPAM-*g*-DMAEMA) undergoes the formation of micellar aggregates consisting of the condensed PNIPAM core and the stretched corona of PDMAEMA and PEG chains.

Through dynamic light scattering, we studied the stimulus-response behavior of block-brush PEG-*b*-P(NIPAM-*g*-DMAEMA) at different temperatures and pHs. Fig. 5 shows the temperature dependence of the scattering intensity of PEG-*b*-P(NIPAM-*g*-

Table 2
Main variations of chemical shift and integrate ratio in ^{1}H NMR spectra of PEG-*b*-P(NIPAM-*g*-DMAEMA) with temperature and solvent.

Proton signal	$CDCl_3$/25 °C	D_2O/25 °C	D_2O/40 °C
$C\underline{H}_2$ in EG[a]	3.66 ppm (1.00)[b]	3.75 ppm (1.00)	3.75 ppm (1.00)
$C\underline{H}(CH_3)_2$ in NIPAM	4.06 ppm (2.18)	3.97 ppm (0.44)	4.09 ppm (0.24)
$OC\underline{H}_2$ in DMAEMA		4.25 ppm (1.75)	4.36 ppm (1.73)
$C\underline{H}_2N(CH_3)_2$ in DMAEMA	2.59 ppm (1.74)	2.81 ppm (1.73)	2.82 ppm (1.71)
$CH_2N(C\underline{H}_3)_2$ in DMAEMA	2.27 ppm (5.21)	2.41 ppm (5.22)	2.40 ppm (5.20)

[a] The integrate of methylene protons of PEG is taken as unity.
[b] The value in the brackets stands for the relative integration of the signal.

DMAEMA) aqueous solution at pH = 5.0, 7.0 and 9.0. In acidic aqueous solution with pH = 5.0, PEG-*b*-P(NIPAM-*g*-DMAEMA) shows weak thermo-response. The solution remains transparent even at 40 °C while hydrodynamic radius (R_h) is not obtained due to the sharp fluctuation in scattering intensity during DLS measurement.

As reported previously, PEG-*b*-PNIPAM aqueous solution exhibited obvious thermo-response at the temperature of 40 °C [45]. The reason for our observation may be explained as followed. Firstly, the protonization degree of PDMAEMA units is high and PDMAEMA chains have better solubility in water at low pH value since p*K*a of PDMAEMA is 7.0. Thus, the steric hindrance of stretching PDMAEMA chains would prevent PEG-*b*-P(NIPAM-*g*-DMAEMA) molecules from inter-molecular aggregation to large micelles. At the same time, PDMAEMA chains are positively charged and their electric repulsion between PDMAEMA chains would have the same effect. In this case, PEG-*b*-P(NIPAM-*g*-DMAEMA) molecules tend to form unimer micelles by the intra-molecular collapse of PNIPAM chains. Moreover, better hydrophilicity of PDMAEMA chains with higher protonization leads to the increase of PNIPAM LCST.

When pH increases to 7.0, PDMAEMA becomes partially deprotonated and less hydrophilic. The decrease of electric repulsion between PDMAEMA chains offers PNIPAM chains the possibility to aggregate inter-molecularly above LCST [46]. Thus, block-brush copolymer shows obvious thermo-response and its LCST gets down to 34 °C. When pH increases to 9.0, PDMAEMA chains turn highly deprotonated, so LCST of block-brush copolymer further decreases to 28 °C, even lower than LCST of homo-PNIPAM. The variation tendency of LCST is consistent with the decrease of PDMAEMA hydrophilicity as the aqueous solution turns less and less acidic. The result clearly demonstrates that PEG-*b*-P(NIPAM-*g*-

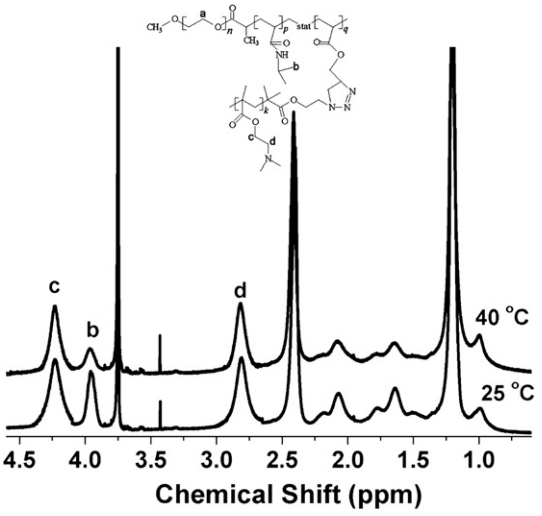

Fig. 4. ^{1}H NMR spectra of PEG-*b*-P(NIPAM-*g*-DMAEMA) in D_2O at 25 °C (low) and 40 °C (up).

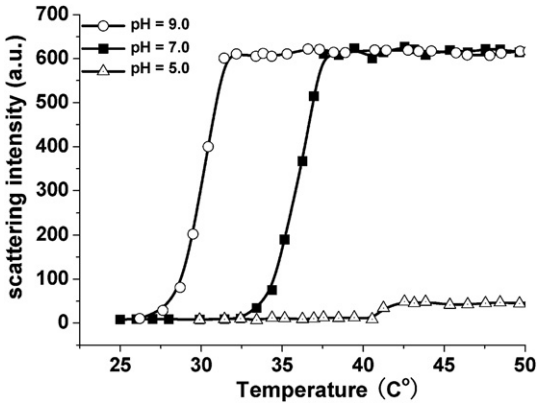

Fig. 5. Variation of DLS scattering intensity of PEG-*b*-P(NIPAM-*g*-DMAEMA) aqueous solution (0.1 mg/mL) at a fixed scattering angle of 30° at different pHs.

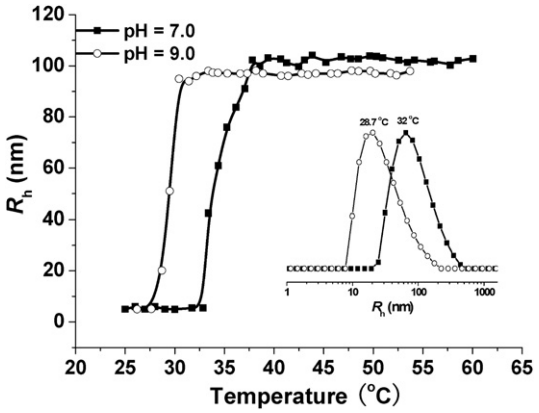

Fig. 6. Temperature dependence of R_h of PEG-*b*-P(NIPAM-*g*-DMAEMA) micelles in aqueous solution (0.1 mg/mL) during the heating process at pH = 7.0 and 9.0. The inseted is the hydrodynamic diameter distribution of PEG-*b*-P(NIPAM-*g*-DMAEMA) micelles at 28.7 and 32.0 °C (pH = 9.0).

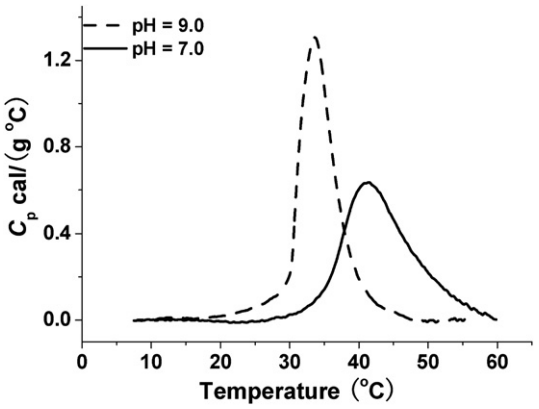

Fig. 8. Temperature dependence of the specific heat capacity (C_p) of PEG-*b*-P(NIPAM-*g*-DMAEMA) aqueous solution (2.0 mg/mL) at pH = 7.0 and 9.0 during the heating process. The heating rate was 1.0 °C/min.

DMAEMA) has both pH and thermal responsive behavior, and LCST of PEG-*b*-P(NIPAM-*g*-DMAEMA) can be modulated by pH value of aqueous solution.

Fig. 6 shows the temperature-dependent of hydrodynamic radius (R_h) of block-brush PEG-*b*-P(NIPAM-*g*-DMAEMA) in aqueous solution (0.1 mg/mL) at two pHs. At pH = 7.0 and 9.0, R_h of copolymer solution increases from about 5 nm for individual block-brush molecule to 90–100 nm for the micelles of inter-molecular aggregation above LCST. The observed value of LCST decreases with the increase of pH. The inset in Fig. 6 shows typical hydrodynamic radius distributions of block-brush copolymer at two temperatures for pH = 9.0. The averaged hydrodynamic radius of block-brush copolymer micelles is 25 and 82 nm at 28.7 and 32.0 °C, respectively. The result should be ascribed to the collapse and aggregation of PINIPAM chains during phase transition. However, even at 55 °C and pH = 9.0, the phase transition concerning with PDMAEMA is not observed.

Transmittance of PEG-*b*-P(NIPAM-*g*-DMAEMA) aqueous solution (2 mg/mL) at three pHs was measured in the temperature range of 20–50 °C. As shown in Fig. 7, PEG-*b*-P(NIPAM-*g*-DMAEMA) aqueous solution (pH = 5.0) keeps transparent almost without the decrease in transmittance, suggesting no formation of large-sized aggregates of PEG-*b*-P(NIPAM-*g*-DMAEMA) at this pH value. With the increase of pH to 7.0 and 9.0, obvious decrease in transmittance is observed, which is contributed to the formation of large inter-molecular micelles. LCST shifts from 33.5 °C at pH = 7.0 to 28.1 °C at pH = 9.0 while the phase transition becomes sharp at pH = 9.0.

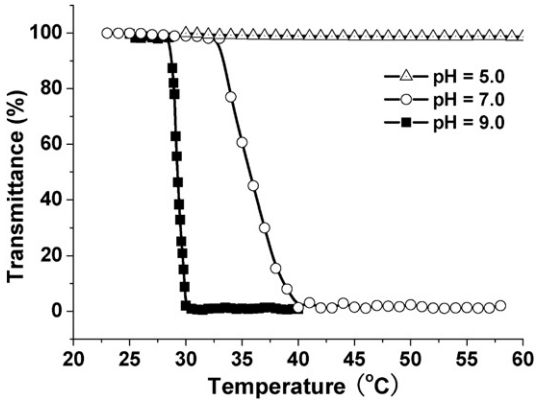

Fig. 7. Transmittance change of PEG-*b*-P(NIPAM-*g*-DMAEMA) aqueous solution (2 mg/mL) with temperature.

Micro-DSC analysis is further employed to investigate the thermal phase transition of PEG-*b*-P(NIPAM-*g*-DMAEMA) block-brush copolymer in the aqueous solutions with a concentration of 2.0 mg/mL at pH = 7.0 and 9.0, and the results are shown in Fig. 8. It is obviously seen that the endothermic peak of block-brush copolymer in the aqueous solution with pH = 7.0 is much broader than that with pH = 9.0. Moreover, the onset temperature of C_p increase is 28.0 and 34.0 °C for pH = 7.0 and 9.0, respectively, indicating the decrease of phase transition temperature of PEG-*b*-P(NIPAM-*g*-DMAEMA) with the increase of pH value. These results are in good agreement with DLS analysis and turbidimetry measurement. It has been reported that the enthalpy change for linear PNIPAM chains is independent of its chain length, and enthalpy change (ΔH) is in the range of 5.5–7.5 kJ/mol [47,48]. The values of ΔH for PNIPAM phase transition at pH = 9.0 and 7.0 is 5.61 kJ/mol and 3.67 kJ/mol in our case, respectively. It should be noted that ΔH value for PNIPAM phase transition at pH = 7.0 is smaller than linear PNIPAM. This is because hydrophilic PEG and PDMAEMA segments tend to solubilize PNIPAM segment and increase LCST of block-brush copolymer. In other words, not all of the PNIPAM units take part in the rupture of hydrogen-bonding with water during thermal transition [49]. When pH is 9.0, PDMAEMA chains are highly deprotonated and show little influence on enthalpy change for PNIPAM chains. At pH = 5.0, PDMAEMA is highly protonated, leading to the hardly observation of C_p change.

4. Conclusions

Block-brush copolymer, poly(ethylene glycol)-*b*-poly[*N*-isopropylacrylamide-*g*-2-(dimethylamino)ethyl methacrylate], was synthesized successfully by the combination of ATRP and click chemistry. Because of the controlled features of ATRP and high efficiency of click chemistry, the obtained block-brush copolymer has well-defined chemical structure, which is confirmed by GPC, ^{1}H NMR and FTIR. PEG-*b*-P(NIPAM-*g*-DMAEMA) exhibits pH and thermal dual responsive behavior. The combination of temperature-varied NMR, DLS, turbidimetry and micro-DSC reveals that the thermal responsive behavior of PEG-*b*-P(NIPAM-*g*-DMAEMA) depends on pH value. At acidic condition, PEG-*b*-P(NIPAM-*g*-DMAEMA) shows weak thermal response and the phase transition of PNIPAM segment may lead to the formation of uni-molecular micelles. At neutral or basic condition, PEG-*b*-P(NIPAM-*g*-

DMAEMA) exhibits strong thermal response and may form the micelles of inter-molecular aggregates. LCST of PEG-*b*-P(NIPAM-*g*-DMAEMA) increases with pH decrease.

Acknowledgments

The financial supports of China Science and Technology Ministry (2007CB936401), HK Earmarked Research Grant (403706) and Key Project of NSFC (20934005) are greatly acknowledged. W-T Li, K-R Zhang and H Zhang thank the support of National Undergraduate Innovative Experiment Project of China Education Ministry and the conveniences of measurements offered by Chemistry Experiment Center of USTC.

References

[1] Discher DE, Eisenberg A. Science 2002;297:967–73.
[2] Zhang LF, Eisenberg A. Science 1995;56:1728–31.
[3] Talingting MR, Munk P, Webber SE, Tuzar Z. Macromolecules 1999;32:1593–601.
[4] Yamato M, Akiyama Y, Kobayashi J, Yang J, Kikuchi A, Okano T. Prog Polym Sci 2007;32:1123–33.
[5] Kim TH, Huh J, Hwang J, Kim HC, Kim SH, Sohn BH, et al. Macromolecules 2009;42:6688–97.
[6] Cui HG, Chen ZY, Zhong S, Wooley KL, Pochan DJ. Science 2007;317:647–50.
[7] Yu K, Eisenberg A. Macromolecules 1996;29:6359–61.
[8] Martin TJ, Prochazka K, Munk P, Webber SE. Macromolecules 1996;29:6071–3.
[9] Reddy TT, Takahara A. Polymer 2009;50:3537–46.
[10] Weber C, Becer CR, Hoogenboom R, Schubertt US. Macromolecules 2009;42:2965–71.
[11] Teertstra SJ, Gauthier M. Macromolecules 2007;40:1657–66.
[12] Wang JS, Matyjaszewski K. Macromolecules 1995;28:7901–10.
[13] Chiefari J, Chong YK, Ercole F, Krstina J, Jeffery J, Le TPT, et al. Macromolecules 1998;31:5559–62.
[14] Roos SG, Muller AHE, Matyjaszewski K. Macromolecules 1999;32:8331–5.
[15] Shinoda H, Matyjaszewski K. Macromolecules 2001;34:6243–8.
[16] Zhang ZB, Shi ZQ, Han X, Holdcroft S. Macromolecules 2007;40:2295–8.
[17] Tornoe CW, Christensen C, Meldal M. J Org Chem 2002;67:3057–64.
[18] Diaz DD, Punna S, Holzer P, McPherson AK, Sharpless KB, Fokin VV, et al. J Polym Sci A Polym Chem 2004;42:4392–403.
[19] Vora A, Singh K, Webster DC. Polymer 2009;50:2768–74.
[20] Petrova S, Riva R, Jerome C, Lecomte P, Mateva R. Eur Polym J 2009;45:3442–50.
[21] Liu JQ, Tao L, Xu JT, Jia ZF, Boyer C, Davis TP. Polymer 2009;50:4455–63.
[22] Bernard J, Favier A, Davis TP, Barner-Kowollik C, Stenzel MH. Polymer 2006;47:1073–80.
[23] Gungor E, Durmaz H, Hizal G, Tunca U. J Polym Sci A Polym Chem 2008;46:4459–68.
[24] Shi GY, Pan CY. J Polym Sci A Polym Chem 2009;47:2620–30.
[25] Chen CP, Kim JS, Liu DJ, Rettig GR, McAnuff MA, Martin ME, et al. Bioconjugate Chem 2007;18:371–8.
[26] Nuopponen M, Ojala J, Tenhu H. Polymer 2004;45:3643–50.
[27] Cai T, Marquez M, Hu ZB. Langmuir 2007;23:8663–6.
[28] Zhang WQ, Shi LQ, Wu K, An YG. Macromolecules 2005;38:5743–7.
[29] You YZ, Oupicky D. Biomacromolecules 2007;8:98–105.
[30] Xu YY, Bolisetty S, Drechsler M, Fang B, Yuan JY, Ballauff M, et al. Polymer 2008;49:3957–64.
[31] Jiang X, Lok MC, Hennink WE. Bioconjugate Chem 2007;18:2077–84.
[32] Auguste DT, Armes SP, Brzezinska KR, Deming TJ, Kohn J, Prud'homme RK. Biomaterials 2006;27:2599–608.
[33] Manickam DS, Oupicky D. Bioconjugate Chem 2006;17:1395–403.
[34] Ciampoli M, Nardi N. Inorg Chem 1966;5:41.
[35] Li J, He WD, Han SC, Sun XL, Li LY, Zhang BY. J Polym Sci A Polym Chem 2009;47:786–96.
[36] Xu ZS, Hu XX, Li XQ, Yi CF. J Polym Sci A Polym Chem 2008;46:481–8.
[37] Masci G, Giacomelli L, Crescenzi V. Macromol Rapid Commun 2004;25:559–64.
[38] Beers KL, Gaynor SG, Matyjaszewski K, Sheiko SS, Moller M. Macromolecules 1998;31:9413–5.
[39] Neugebauer D, Zhang Y, Pakula T. J Polym Sci A Polym Chem 2006;44:1347–56.
[40] Riess G. Prog Polym Sci 2003;28:1107–70.
[41] Lowe AB, Billingham NC, Armes SP. Chem Commun 1997;11:1035–6.
[42] Butun V, Armes SP, Billingham NC. Polymer 2001;42:5993–6008.
[43] Triftaridou AI, Vamvakaki M, Patrickios CS. Polymer 2002;43:2921–6.
[44] You YZ, Zhou QH, Manickam DS, Wan L, Mao GZ, Oupicky D. Macromolecules 2007;40:8617–24.
[45] Tang XD, Liang XC, Yang Q, Fan XH, Shen ZH, Zhou QF. J Polym Sci A Polym Chem 2009;47:4420–7.
[46] Xu XW, Liu C, Huang JL. J Appl Polym Sci 2008;108:2180–8.
[47] Shibayama M, Mizutani S, Nomura S. Macromolecules 1996;29:2019–24.
[48] Shan J, Chen J, Nuopponen M, Tenhu H. Langmuir 2004;20:4671–6.
[49] Li LY, He WD, Li J, Han SC, Sun XL, Zhang BY. J Polym Sci A Polym Chem 2009;47:7066–77.